Article

Computational Studies on Microreactors for the Decomposition of Formic Acid for Hydrogen Production Using Heterogeneous Catalysts

Eleana Harkou [1] , Panayiota Adamou [1], Kyproula Georgiou [1], Sanaa Hafeez [2], Sultan M. Al-Salem [3] , Alberto Villa [4] , George Manos [5] , Nikolaos Dimitratos [6,7] and Achilleas Constantinou [1,*]

1   Department of Chemical Engineering, Cyprus University of Technology, 57 Corner of Athinon and Anexartisias, Limassol 3036, Cyprus; ea.harkou@edu.cut.ac.cy (E.H.); paa.adamou@edu.cut.ac.cy (P.A.); ks.georgiou@edu.cut.ac.cy (K.G.)
2   School of Engineering and Materials Science, Queen Mary University of London, London E14NS, UK; sanaa.hafeez@qmul.ac.uk
3   Environmental & Life Sciences Research Centre, Kuwait Institute for Scientific Research, P.O. Box 24885, Safat 13109, Kuwait; ssalem@kisr.edu.kw
4   Dipartimento di Chimica, Universitá degli Studi di Milano, via Golgi, 20133 Milan, Italy; alberto.villa@unimi.it
5   Department of Chemical Engineering, University College London, London WCIE7JE, UK; g.manos@ucl.ac.uk
6   Dipartimento di Chimica Industriale "Toso Montanari", Alma Mater Studiorum Università di Bologna, Viale Risorgimento 4, 40136 Bologna, Italy; nikolaos.dimitratos@unibo.it
7   Center for Chemical Catalysis-C3, Alma Mater Studiorum Università di Bologna, Viale Risorgimento 4, 40136 Bologna, Italy
*   Correspondence: a.konstantinou@cut.ac.cy

Abstract: Sustainable alternatives to conventional fuels have emerged recently, focusing on a hydrogen-based economy. The idea of using hydrogen (H_2) as an energy carrier is very promising due to its zero-emission properties. The present study investigates the formic acid (FA) decomposition for H_2 generation using a commercial 5 wt.% Pd/C catalyst. Three different 2D microreactor configurations (packed bed, single membrane, and double membrane) were studied using computational fluid dynamics (CFD). Parameters such as temperature, porosity, concentration, and flow rate of reactant were investigated. The packed bed configuration resulted in high conversions, but due to catalyst poisoning by carbon monoxide (CO), the catalytic activity decreased with time. For the single and double membrane microreactors, the same trends were observed, but the double membrane microreactor showed superior performance compared with the other configurations. Conversions higher than 80% were achieved, and even though deactivation decreased the conversion after 1 h of reaction, the selective removal of CO from the system with the use of membranes lead to an increase in the conversion afterwards. These results prove that the incorporation of membranes in the system for the separation of CO is improving the efficiency of the microreactor.

Keywords: hydrogen; formic acid; dehydrogenation; microreactor; membrane; carbon monoxide

1. Introduction

A major contributor to climate change is the combustion of large quantities of fossil fuels in the energy sector. Therefore, providing sustainable alternatives to conventional fuels is gaining attention in industrial circles and becoming mandatory in scientific fields of research. All of which are attempting to stabilize the harmful environmental effects of fossil fuels [1]. The key is to find a back-up source that is secure, renewable, and internationally available. Hydrogen (H_2) is a naturally abundant, clean, and renewable energy source that can be exploited as an energy carrier and a potential transportation fuel. It is an emission-free energy carrier and can be produced through numerous paths such as thermochemical

(TC) and biological processes, electrolysis, and photolysis [2]. The transition, from a fossil fuel-based economy to a hydrogen-market faces many technical and socioeconomic hurdles that hinder the implementation of H_2 as a future energy source [3].

Instead of H_2, liquid organic hydrogen carriers (LOHCs) can be utilized. Formic acid (FA/CH_2O_2) is a great example of a LOHC. It can be generated by the hydrogenation of carbon dioxide (CO_2), and its decomposition takes place in mild conditions. It is a safe option to transport and store when compared with H_2. FA can contain up to 4.4 wt.% of H_2, which is double than the content of compressed H_2 at a pressure of 350 bar at the same volume, and an energy density of 2.1 kWh/L [4]. FA can be decomposed via two pathways as depicted in Equations (1) and (2). The first, which is the more desirable reaction, includes the decarboxylation towards CO_2 and H_2. The second pathway, the undesirable route, is the decarbonylation towards carbon monoxide (CO) and water (H_2O) and must be avoided due to the formation of CO, which poisons and deactivates the catalyst [5]. The co-product, CO_2, of the decomposition of FA can be converted back into FA, either electrochemically or through catalytic hydrogenation, promoting a circular energy economy with net-zero CO_2 emissions released into the atmosphere [6,7]. In addition, FA can be derived from plant biomass processing, promoting renewability of the H_2 from this technology with significant developments in the recent years for the sustainable production of FA from lignocellulosic biomass [8].

$$HCOOH(l) \ \rightarrow CO_2 + H_2 \tag{1}$$

$$HCOOH(l) \ \rightarrow CO + H_2O \tag{2}$$

CO binds strongly with the metal center of catalysts causing a good fraction of it to deactivate. It also poisons Proton Exchange Membranes (PEM) of fuel cells [9,10]. The undesirable CO formation can be limited by the appropriate selection of suitable catalysts. Heterogeneous and homogenous catalysts can be used for the decomposition of FA, with the former being preferable. Homogeneous catalysts are more stable and are an option that is hard to separate from the mixture and reuse it. Conversely, heterogeneous catalysts offer various advantages including reusability, recyclability, and that they can be shaped into different geometries [11,12]. Among the heterogeneous catalysts investigated for the decomposition of FA, the Pd- and Au-based catalysts as well as their bimetallic materials are considered the most effective materials for this reaction [13,14], favoring the production of H_2 against the formation of CO [15]. Choi et al. [16] developed palladium–silver (Pd.Ag) alloy cores with thin Pd shells as a catalyst for efficient H_2 production from FA decomposition in an aqueous solution. The catalytic activity of PdAg@Pd ONCs toward FA decomposition was optimal, achieving at 50 °C a turnover frequency (TOF) of 21,500 h^{-1}. Gas chromatography (GC) was used to detect CO contamination where the selective H_2 generation was confirmed. Further studies on the catalyst disclosed that the atomic ratio of Pd/Ag and the atomic layer of Pd shells. The results clearly demonstrated that the approach of core–shell engineering is effective for the efficient development of catalysts to generate H_2 from FA, with no contamination of CO. Zhang et al. [17] synthesized ruthenium (Ru) catalysts supported on two different porous organic polymers (POPs). Ru@POPs-TPP had a low activity and a significant amount of CO in the products ($\approx$2.221%). The Ru@POPs-PPh3 catalyst exhibited an excellent activity with 7284 h^{-1} of TOF value. Even though the surface areas of the two catalysts were similar, their catalytic performance was significantly different. The Fourier transform infrared (FT-IR) spectra showed that the properties of ligands in the polymer framework may influence the overall performance of the catalysts.

Experimental data and density functional theory (DFT) analysis were combined by Barlocco et al. [18], in order to investigate the role of Au in enhancing the selectivity and activity of Pd catalysts for FA decomposition. Monometallic Pd and Au catalysts were also investigated and showed lower catalytic activities than Pd.Au alloy catalysts, confirming the superiority of a bimetallic catalytic system. The optimal performance was exhibited

by the 1%PD$_6$Au$_4$@HHT catalyst (TOF 3539 h^{-1}). Monometallic Pd catalyst was found to deactivate due to leaching and CO poisoning while 1%PD$_6$Au$_4$@HHT resulted in excellent stability after six continuous runs.

Over the years, different reactor types and set-ups were utilized for the catalytic decomposition of FA. The most common and studied systems are packed bed reactors, knowing that they are significant for heterogeneous catalysis [15,19,20]. Batch reactors were also evaluated for this reaction [21], but continuous stirred tank reactors were more preferable due to their ability to produce a stable and continuous stream of H$_2$ for fuel cell implementations. Also, microchannel reactors have gained lot of attention due to their high efficiency and in situ H$_2$ supply but still high-performance microreactors for FA decomposition are not developed for large-scale applications [22,23]. Membrane technology may also be used for the catalytic decomposition of FA. Membranes offer the ability to selectively separate different reaction components within the reactor. The introduction of a membrane into the continuous flow system can improve the performance of the reaction by removing the CO formed during the process. A membrane reactor can operate at the same time for reactions and separation of various components reducing significantly the cost of a process [24]. Recovery of products and purification of H$_2$ can occur in a single unit providing the opportunity to improve efficiency and lower the cost. The most developed membranes for separating H$_2$ are polymeric membranes due to their better permeability and mild operating conditions, and they have been already applied at a commercial scale. Another type of membranes are dense metal membranes, usually from palladium (Pd), nickel (Ni), platinum (Pt), and their alloys. Their structure allows the selective diffusion of H$_2$ while rejecting other gases. Pd-based membranes are the most studied, but their high cost limits their application and practicality [25]. A tubular membrane reactor for the catalytic decomposition of ammonia (NH$_3$) was employed by Cechetto et al. [26]. A Ru-based catalyst was used with double-skin Pd membranes. Results were compared with that of a packed bed reactor which indicated that the membrane enhances the overall performance of the reactor, achieving higher conversions. Above 425 °C, a conversion of 100% was observed with 86% H$_2$ recovery of 99.998% purity.

Hafeez et al. [27] investigated a novel microreactor configurations for FA decomposition with the use of a 5 wt.% Pd/C catalyst. Computational methods were used to evaluate the experimental data. Results showed that the packed bed and coated wall microreactors achieved a comparable performance with each other, with the coated wall configuration being slightly superior. The membrane microreactor exhibited the best performance compared with other microreactors given the fact that the deactivation from CO formation was alleviated with the use of a membrane.

In previous works carried out by our group [20], considering the formic acid decomposition using the Pd/C catalyst, the investigation was firstly carried out in batch and continuous flow reactors where experimental and theoretical studies took place. The formation of CO and herein the deactivation of the catalyst due to poisoning were a challenge we tried to minimize to ppm level. Different reactor configurations considering continuous flow reactors were studied to eliminate the production of CO [27].

Main aim of the work is to investigate and study different parameters in order to enhance the conversion of formic acid and the removal of CO, which inhibits the reaction, by using membrane configurations and therefore to improve stability of the catalyst. In the present work, CFD analysis was conducted on a packed bed, single and double membrane microreactors for FA decomposition with the use of commercial 5 wt.% Pd/C catalyst offering for the first time a reasonable, effective solution on the efficient removal of CO. Process simulation modeling using computational fluid dynamics (CFD) is valuable for a reaction system as it gives significant information regarding various parameters on different reactor configurations that can be validated from experimental data [20,27–33].

2. Results and Discussion

2.1. Packed Bed Microreactor

In this section, the obtained results from the modelling of the packed bed are presented. The validity of the model was examined by our group in a previous study [20]. The FA reaction occurred at 1 bar of pressure and at an initial flow rate of 0.05 mL/min in the presence of Pd/C catalyst. The commercial Pd/C catalyst showed a 99.9% selectivity for H_2, and the characterization and techniques used can be found in a previous work [34]. The small quantity of CO produced is significant to affect the stability of the catalyst, as it leads to the poisoning of the catalyst. Figure 1 shows the effect of temperature on the FA conversion. The conversion of FA is determined as the mass balance of FA in the reactor $((F_{FA,in} - F_{FA,out})/F_{FA,in})$. The FA reaction was investigated at 30, 40, 50, and 60 °C. An increase in the conversion was expected as the temperature rises due to the Arrhenius expression (where $k = A·exp(-E_a/RT)$). In contrast, the obtained results showed that the increase in the reaction temperature leads to lower FA conversion values. It is assumed that at higher temperatures the favorable reaction is the one producing CO, which may poison the catalyst, and according to the literature, Pd-based catalysts are deactivated by the production of CO [35]. As a result, catalyst's activity will decrease, as well as the conversion of the reaction. Moreover, Sanchez et al. [34] showed in the past that the possible cause of the deactivation of this catalyst might be the production of CO, and with this theoretical study, we aimed to improve the deactivation. Kosider et al. [36] investigated the FA decomposition in a batch reaction using a Pd/C catalyst showing similar trend in the results as our findings. Their results showed a decrease in FA conversion with an increase in temperature. The activity of the catalyst was found to be lower at higher temperatures as well, revealing the poisoning and deactivation of the catalyst from the production of CO.
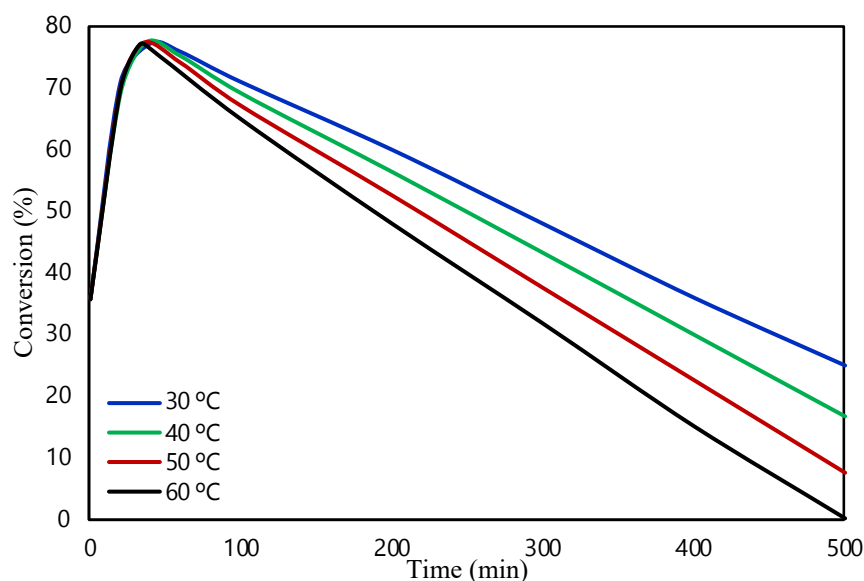
Figure 1. Temperature effect on FA conversion in packed bed microreactor.

Figure 2 shows the catalyst porosity effect on the reaction's conversion. Three different porosities of the catalyst were studied, 0.4, 0.5, and 0.6, at 30 °C, achieving the same conversion at the first 50 min approximately of the reaction. After the first 50 min of the reaction, it can be observed from the figure that there is a decrease in the conversion due to the poisoning of the catalyst since the activity of the catalyst is decreased because of the generation of CO. Moreover, higher the porosity of the catalyst, better the performance and the conversion of FA within the microreactor. This can be attributed to the fact that at higher catalyst porosities, the distribution of active sites on the surface of the catalyst could be higher, therefore leading to the increase in the adsorption of FA.
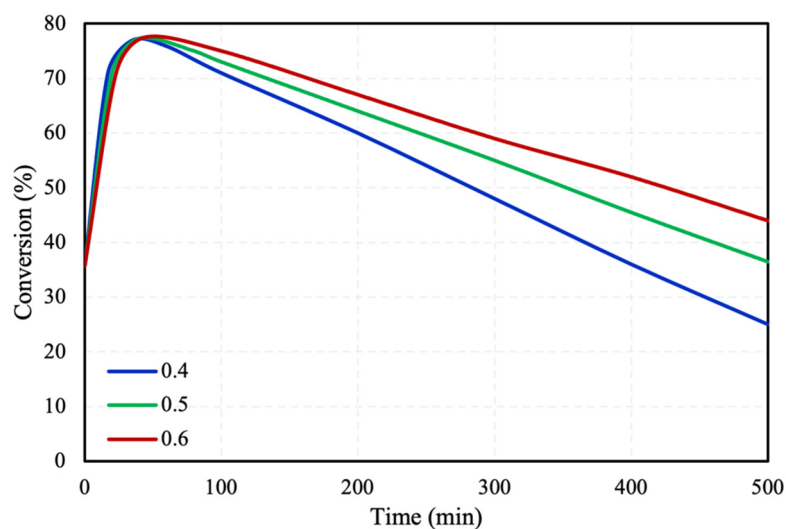
Figure 2. Catalyst porosity effect on FA conversion in packed bed microreactor.

The FA inlet flow rate was investigated for its effect on the conversion. Three different inlet flow rates were studied (i.e., 0.05, 0.07, and 0.09 mL/min) at 30 °C, with the results presented in Figure 3. It can be observed from the figure that with lower inlet flow rates, higher FA conversions are achieved. By increasing the inlet flow rate, the velocity of the fluid also increased leading to lower fluid residence time inside the microreactor and herein lower conversion. The Particle Tracing Module offered by COMSOL was used in order to calculate the fluid residence time inside the microreactor. Figure 4 presents the distribution of residence time of the fluids inside the microreactor at the three investigated flow rates. It is observed that the residence time of the flow rates of 0.05, 0.07, and 0.09 mL/min are 6.28, 4.49, and 3.49 min, respectively. The figures reveal that at higher flow rates the fluid residence time inside the microreactor is lower, leading to lower FA conversions.
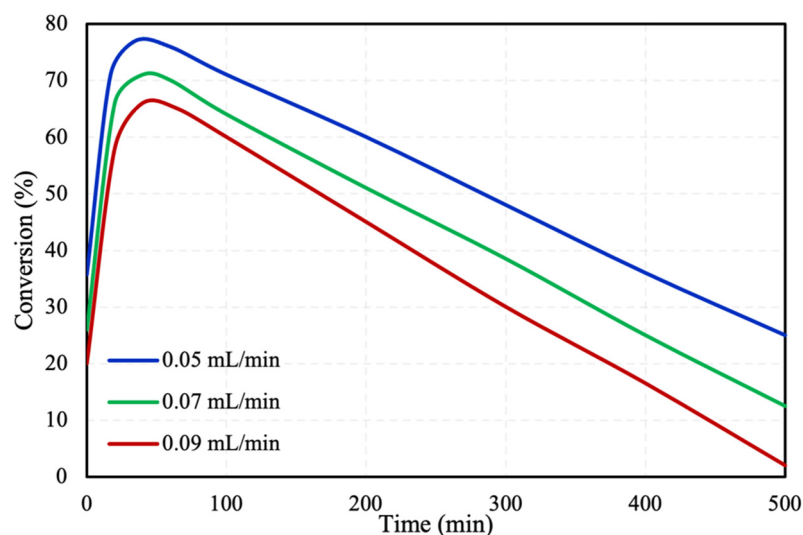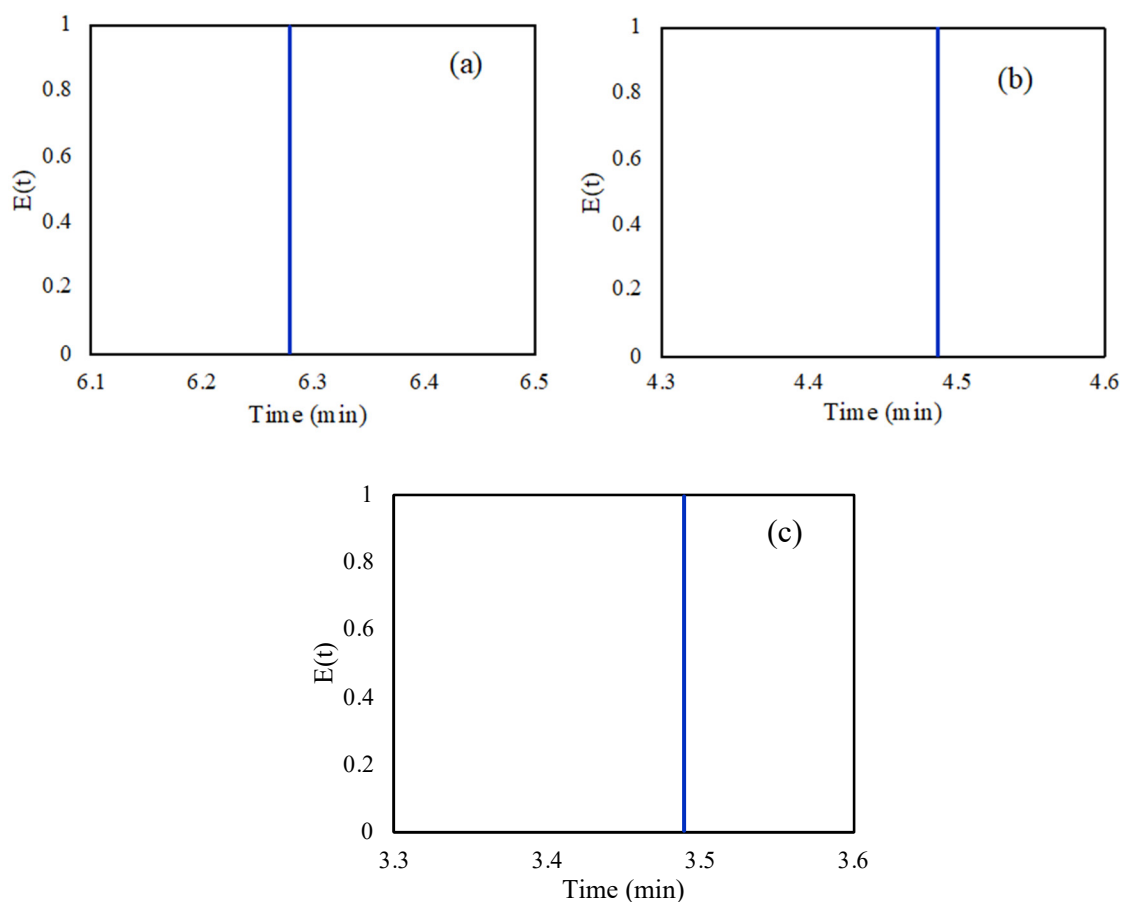

Figure 3. FA initial flow rate effect on FA conversion in packed bed microreactor.

Figure 4. Residence time distribution at (**a**) flow rate of 0.05 mL/min, (**b**) 0.07 mL/min, and (**c**) 0.09 mL/min in the packed bed microreactor.

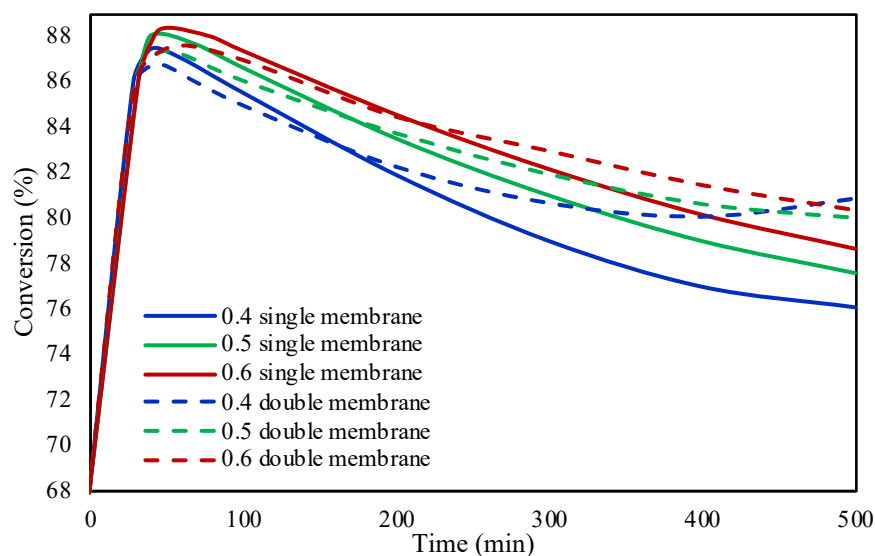### 2.2. Single and Double Membrane Packed Bed Microreactor

In this section, the single and double membrane packed bed microreactor were investigated to improve the performance of the microreactor and hence the conversion of FA using the commercial Pd/C catalyst. The membrane was introduced in the model to selectively remove and separate the CO from the other gas fluids and to avoid the catalyst poisoning. Figure 5 presents the comparison of the conversion of FA within the single and double membrane configurations at different reaction temperatures. The single membrane is selectively removing the CO from the one side of the microreactor (see reactor configurations in Materials and Methods Section 3) while the removal of CO is enhanced at the double membrane microreactor where the CO is removed from both sides. It was also observed that the double membrane microreactor showed better performance than the single due to the more efficient removal of CO from the microreactor. The selective removal of CO prevented and minimized the deactivation of the catalyst with respect to time, and herein, the performance and conversion of the microreactor was improved. Lastly, it was revealed in the double membrane configuration that by removing CO from the system, the conversion tends to increase, while increasing the temperature, the deactivation of the catalyst is minimized. Hafeez et al. [27] showed that the removal of CO using a single membrane microreactor inhibits and minimizes the deactivation of the catalyst. Sandoval and Gigola [37] revealed through the TPD profile that the adsorption of CO from the surface of the active sites changes from the favored multiple coordinated strong form to the weak, indicating that species such as the CO tend to desorb at higher temperatures (>60 °C). Therefore, the simultaneous combination of the efficient removal of CO using membranes and the removal of the adsorbed CO from the active sites as the temperature of the reactor increases is responsible for the enhanced stability of the catalyst.
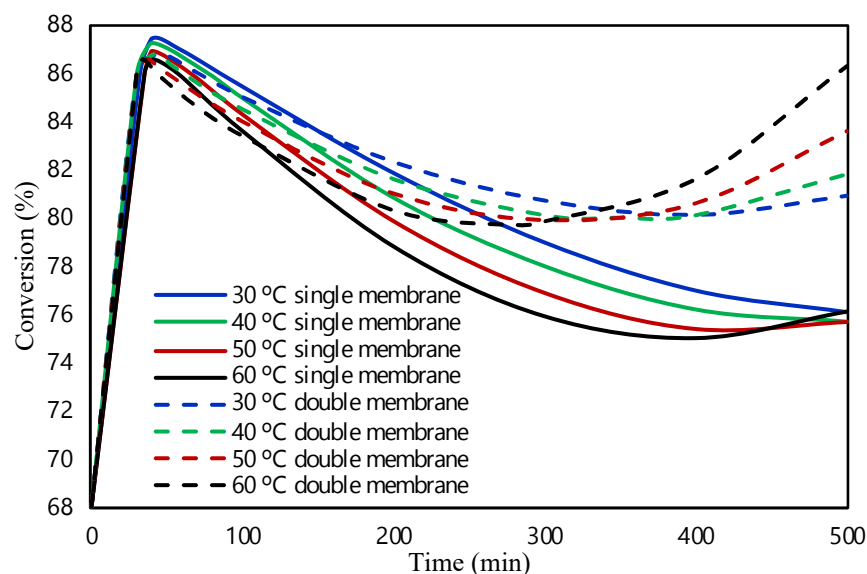
Figure 5. Comparison between the single and double membrane configurations on the formic acid conversion at different temperatures.

Figure 6 shows the effect of catalyst's porosity on FA conversion in both membrane configurations at 30 °C. The three different investigated catalyst porosities of 0.4, 0.5, and 0.6 showed similar trend as the investigation in the packed bed microreactor. The conversion during the first 40 min is similar, while due to the poisoning of the catalyst the conversion decreases thereafter. The membrane configurations showed an increase in the conversion while increasing the catalyst porosity, likewise in the case of packed bed microreactor. The double membrane microreactor due to better removal efficiency of CO achieved slightly higher conversions of FA in comparison to the single membrane microreactor.

Figure 6. Comparison between the single and double membrane configurations on the formic acid conversion at different catalyst porosities.

The investigation of the flow rate's effect on the FA conversion, at 30 °C, in both single and double membrane microreactors (Figure 7) showed similar results as the packed bed microreactor. The single membrane microreactor is selectively removing CO from the one side of the microreactor (see reactor configurations in Materials and Methods Section 3) while the double membrane microreactor is removing the CO from both sides of the reactor. The three different flow rates of 0.05, 0.07, and 0.09 mL/min revealed that the

increase in the inlet flow rate is leading to lower FA conversions. Similar to the packed bed microreactor investigation, the FA conversion according to the flow rate effect is attributed to the residence time of the fluid inside the microreactor. It was also observed that the efficient removal of CO in the double membrane configuration increased the conversion of FA with respect to time.
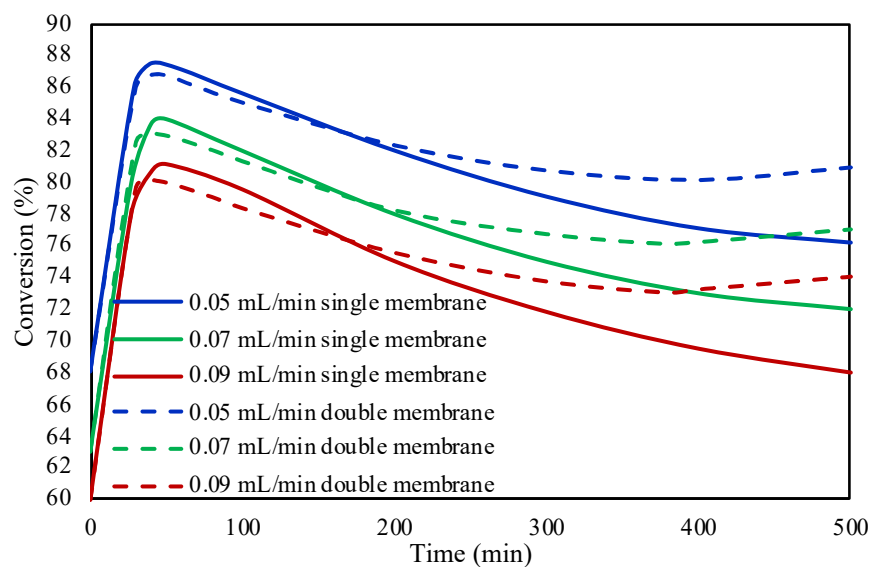
Figure 7. Comparison between the single and double membrane configurations on the formic acid conversion at different inlet flow rates.

In this work, we also aimed to investigate the influence of FA concentration on the conversion in the double membrane microreactor. Three different FA concentrations were studied, 0.5, 0.7, and 0.9 mol/m^3 at 30 °C. Figure 8 presents the concentration effect of FA on the reaction conversion. It was observed that by increasing the FA concentration higher conversions are achieved with respect to time. The increase in the concentration leads to higher reaction rates as there is a correlation between the reaction rate and the FA concentration according to the reaction rate.
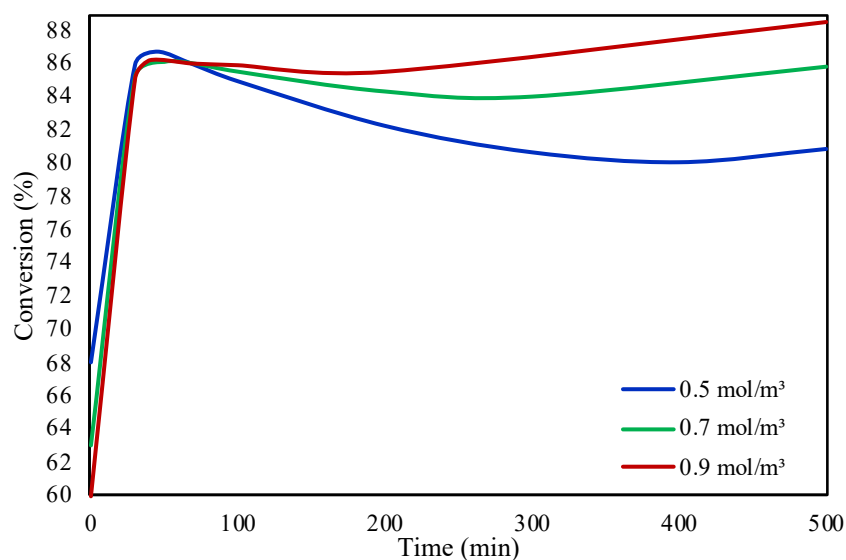
Figure 8. FA concentration effect on the conversion of FA in the double membrane microreactor.

3. Materials and Methods

3.1. Modelling Methodology

In this study, 5 wt.% Pd/C catalyst was used under mild conditions in a packed bed, single membrane, and double membrane microreactors in 2D models for the FA decomposition. A 0.05 mL/min flow rate was used for this study, and the reaction was studied from 30 to 60 °C. CFD modelling studies were implemented to show the behavior between the heterogeneous reaction of particles and fluid within these microreactors. The validity of the model was investigated in a previous work revealing the validity of the designed model [20].

The microreactor configurations were designed as 2D models (Figure 9) hypothesizing that temperature, flow, and mass profiles take place only in the axial and radial directions. The assumptions with which the model was designed include: (i) laminal flow and unsteady state conditions were applied, (ii) only CO can pass through the membrane or membranes, (iii) there are no heat transfer phenomena since isothermal conditions were applied, (iv) the liquid dissolution in the gas phase and in the membrane is considered negligible, and (v) the transport coefficient values and physical properties of the constant axial fluid velocity were uniform. Finally, the membrane material for the selective removal of CO is polytetrafluoroethylene (PTFE).
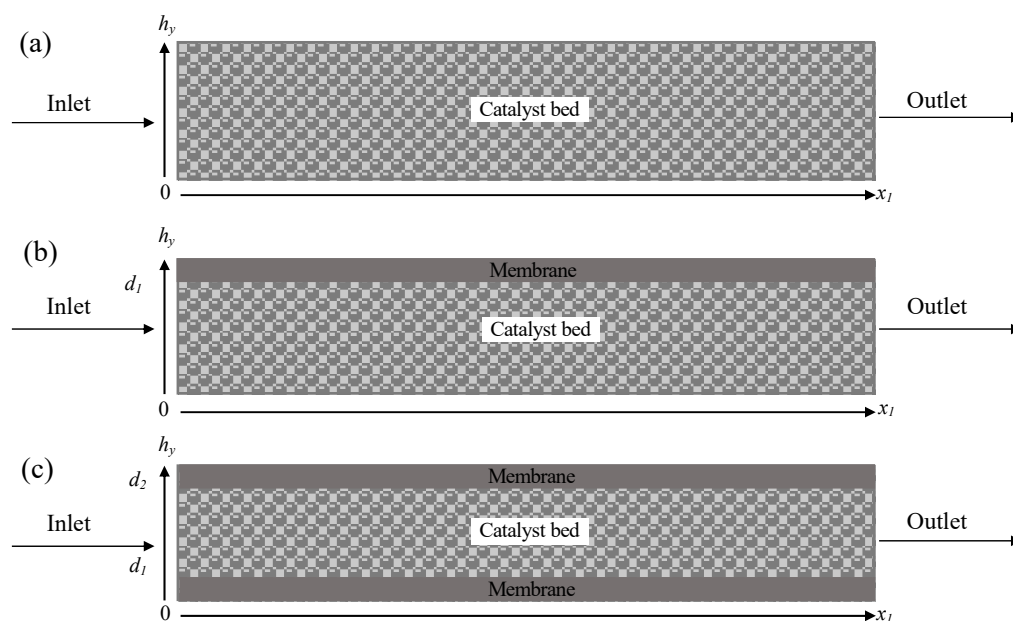
Figure 9. Reactor configurations of (**a**) packed bed, (**b**) single membrane, and (**c**) double membrane microreactors used for this study.

3.2. Reaction Kinetics

The commercial Pd/C catalyst used for the computational investigation was previously examined exhibiting selectivity for H_2 of 99.9% and a TOF value of 1136 h^{-1} at 30 °C for FA decomposition to H_2 and CO_2 [34]. The negligible amount of CO that is produced is significant in order to poison and deactivate the catalyst. The rate of reaction can be expressed as:

$$r = k \times C^n \tag{3}$$

where k and r are the reaction constant and reaction rate, respectively. C is the FA concentration, and n is the reaction order [34].

The activity parameter ($a(t)$) is introduced in the model in order to predict the catalyst activity. This parameter is correlated to the concentration of CO, which is accumulated in the microreactor and poisons the catalyst. The catalyst deactivation and herein the decrease

in the conversion is modelled based on concentration of CO with the activity parameter given as:

$$a(t) = 1 - \lambda \times C_{CO} \tag{4}$$

3.3. Conservation Equations

The equation of the transportation of the species in the catalyst bed is given as:

$$u_x \frac{\delta c_i}{\delta x} = D_{i,A} \frac{\delta^2 c_i}{\delta x^2} + D_{i,T} \frac{\delta^2 c_i}{\delta y^2} - J_i S_b \tag{5}$$

where u_x (m/s) is fluid's velocity in x direction, D_i and J_i are the coefficient of axial dispersion in the axial and transverse directions and the fluid's molar flux in the catalyst, respectively, and S_b is the active specific surface area of particles that is in contact with the reactant components in the catalyst bed and is expressed as:

$$S_b = S_a (1 - \varepsilon) \tag{6}$$

where ε and S_a are the catalyst bed voidage and the catalyst specific surface area (m), respectively [38]. The specific surface area of spherical particles is:

$$S_a = \frac{3}{r_{pe}} \tag{7}$$

where r_{pe} (m) is the catalyst's particle radius.

At the interface of pellet–fluid, the film condition's assumption is made, considering the external mass transfer as a resistance described as:

$$J_i = h_i (c_i - c_{i,ps}) \tag{8}$$

$$h_i = \frac{Sh \cdot D_i}{2 r_{pe}} \tag{9}$$

$$Sc = \frac{\mu}{\rho \cdot D_i} \tag{10}$$

$$Re = \frac{2 r_p \cdot \rho \cdot u_x}{\mu} \tag{11}$$

$$Sh = 2 + 0.552 Re^{1/2} Sc^{1/3} \tag{12}$$

where h_i and $c_{i,ps}$ are the coefficient of external mass transfer and species concentration at catalyst's surface. Sc, ρ, and μ are the Schmidt number, the fluid's density, and viscosity, respectively. Re and Sh are the Reynolds number and the Sherwood number, respectively [39,40].

The reaction is occurring within the catalyst particle combining the feature of Reactive Pellet Bed on COMSOL. Across the spherical shell mass balance of the powdered particle, an extra 1D predefined dimension on the normalized radius $\left(r = r_{dim} / r_{pe} \right)$ is expressed as:

$$4\pi N \left\{ r^2 r_{pe}^2 \varepsilon_{pe} \frac{\partial c_{pe,i}}{\partial t} + \nabla \cdot \left(-r^2 D_{i,eff} \nabla c_{pe,i} \right) = r^2 r_{pe}^2 R_{pe} \right\} \tag{13}$$

where N is particles number, $D_{i,eff}$ is the coefficient of effective diffusion of fluids in the pores of powdered particle, $c_{pe,i}$ and R_{pe} are the concentration of components in the powdered catalyst and the reaction rate term, respectively.

The diffusion coefficients (effective) of species in the particle material are described by the Knudsen or bulk diffusivity expressed as [39]:

$$D_{i,eff} = \frac{D_{i,AB}\Phi_p\sigma_c}{\tau} \tag{14}$$

where $D_{i,AB}$ is the diffusivity of fluid components in bulk, Φ_p is the porosity of the powdered catalyst, and σ_c and τ are the constriction factor and tortuosity, respectively.

The transportation of components through the membrane is described as:

$$D_{i,m}\left(\frac{\delta^2 c_{i,m}}{\delta x^2} + \frac{\delta^2 c_{i,m}}{\delta y^2}\right) = 0 \tag{15}$$

where $c_{i,m}$ and $D_{i,m}$ are the concentration and the species coefficient of diffusion in the membrane.

The Particle Tracing Module is a tool offered by COMSOL to decipher the distribution of residence time by computing the direction of particles. The residence time distribution is an alternative to the first-order Newtonian formulation given as:

$$\frac{dq}{dt} = v \tag{16}$$

where q is the pellet position (m), and v the velocity of the particle (m/s).

The boundary conditions used for investigated microreactor configurations are given as: for packed bed microreactor,

$$\text{at } x = 0; \ c_i = c_{i,in} \tag{17}$$

$$\text{at } x = x_i; \ \frac{\delta c_i}{\delta x} = 0 \tag{18}$$

$$\text{at } y = 0; \ c_i = 0 \tag{19}$$

$$\text{at } r = 1; \ c_{i,p} = c_{i,ps} \tag{20}$$

$$\text{at } r = 0; \ \frac{\delta c_{i,p}}{\delta r} = 0 \tag{21}$$

for single membrane microreactor,

$$\text{at } x = 0; \ c_i = c_{i,in} \tag{22}$$

$$\text{at } x = x_i; \ \frac{\delta c_i}{\delta x} = 0 \tag{23}$$

$$\text{at } y = 0; \ c_i = 0 \tag{24}$$

$$\text{at } r = 1; \ c_{i,p} = c_{i,ps} \tag{25}$$

$$\text{at } r = 0; \ \frac{\delta c_{i,p}}{\delta r} = 0 \tag{26}$$

$$\text{at } y = d_1; \ c_{i,m} = Hc_i \tag{27}$$

$$\text{at } y = h_y; \ c_{i,m} = c_{i,g} \tag{28}$$

and for double membrane microreactor,

$$\text{at } x = 0; \ c_i = c_{i,in} \tag{29}$$

$$\text{at } x = x_i; \ \frac{\delta c_i}{\delta x} = 0 \tag{30}$$

$$\text{at } y = 0; \ c_i = 0 \tag{31}$$

$$\text{at } r = 1; \ c_{i,p} = c_{i,ps} \tag{32}$$

$$\text{at } r = 0; \ \frac{\delta c_{i,p}}{\delta r} = 0 \tag{33}$$

$$\text{at } y = d_1, \ y = d_2; \ c_{i,m} = Hc_i \tag{34}$$

$$\text{at } y = 0, \ y = h_y; \ c_{i,m} = c_{i,g} \tag{35}$$

COMSOL Multiphysics 6.0 was used for this investigation coupling the conservation, mass balance equations, and boundary conditions on a laptop with 32 GB of RAM. A sensitivity analysis of the mesh was performed to study the validity of the CFD study by varying the mesh size. Table 1 shows the mesh sensitivity analysis results varying the mesh quality. It was obtained that the results were mesh independent at all three microreactor configurations as the solution was checked for higher degrees of freedom and the difference between the results was found to be less than 1%. Table 2 consists all the modelling parameters that were used for this study.

Table 1. Mesh sensitivity analysis of the microreactor configurations used in this study.

Mesh Quality	Time to Compute	Elements	Vertices	Boundary Elements	Degrees of Freedom	Max. Conv. Rate (30 min)	Difference
Normal	5 s	98	68	36	996	77.766%	Reference
Fine	5 s	154	100	44	1524	77.752%	−0.0018%
Extra Fine	10 s	1010	564	116	9444	77.720%	−0.041%
Extremely Fine	23 s	4030	2132	232	36,972	77.703%	−0.022%

Table 2. Parameters used for the CFD modelling study.

Symbol	Value	Units	Description
c_{FA}	0.5	$mol \ m^{-3}$	FA inlet concentration
u	0.05	$mL \ min^{-1}$	Volumetric inlet flow rate
x_i	25	mm	Microreactor length
y_i	4	mm	Microreactor height
d_m	1	mm	Membrane thickness
T	303–333	K	Reaction temperature
d_{pe}	4	nm	Catalyst pellet size
ρ	1	$kg \ m^{-3}$	Fluid density
ρ_b	1300	$kg \ m^{-3}$	Catalyst density
ε_0	0.4	-	Clean catalyst porosity
R	8.314	$J \ mol^{-1} \ K^{-1}$	Ideal gas constant

4. Conclusions

In this work, three different microreactor configurations were studied for their performance on FA dehydrogenation using 5 wt.% Pd/C catalyst. This study is offering for the first time a substantial solution for minimizing the poisoning of the catalyst by introducing membranes into the reactor system. The innovative implementation of CO selective membranes allows the removal of CO inhibiting the deactivation of the catalyst. The packed bed microreactor showed good performance only in the first 50 min, at all the investigated temperatures, as the generation of CO poisoned the catalyst and reduced its activity. Also, it was observed that the production of CO is more favorable at higher temperatures as the catalyst deactivation is increased. Main aim of the work was to incorporate a membrane in the microreactor system in order to remove the CO and avoid the catalyst deactivation. The single and double membrane configurations showed better performance in terms of lowering the deactivation of the catalyst with the last one having the best performance. Parametric studies investigating the effect of catalyst porosity on the conversion of FA was performed for all three microreactor configurations, revealing that higher the catalyst porosity is, higher is the conversion, due to higher number of active sites and more enhanced adsorption of FA on the catalyst. The effect of the inlet flow rate of FA showed that lower flow rates tend to have higher conversion rates due to the higher residence time of the fluids inside the microreactor. It also investigated the concentration of FA effect on the conversion in the double membrane microreactor showing that the increase in conversion leads to higher reaction rates according to the rate of the reaction. The efficient removal of CO in the double membrane microreactor had a FA conversion of over 80% in all case studies. Additional 3D studies considering the veritableness of the performance of the microreactors will be performed as future work in order to obtain substantial results. Moreover, the efficient removal of CO by using the specific reactor configurations can be useful as possible solutions for other chemical processes.

References

1. Martins, F.; Felgueiras, C.; Smitkova, M.; Caetano, N. Analysis of fossil fuel energy consumption and environmental impacts in European countries. *Energies* **2019**, *12*, 964. [CrossRef]
2. Amin, M.; Shah, H.H.; Fareed, A.G.; Khan, W.U.; Chung, E.; Zia, A.; Farooqi, Z.U.R.; Lee, C. Hydrogen production through renewable and non-renewable energy processes and their impact on climate change. *Int. J. Hydrogen Energy* **2022**, *47*, 33112–33134. [CrossRef]
3. Stančin, H.; Mikulčić, H.; Wang, X.; Duić, N. A review on alternative fuels in future energy system. *Renew. Sustain. Energy Rev.* **2020**, *128*, 109927. [CrossRef]
4. Bulushev, D.A. Progress in catalytic hydrogen production from formic acid over supported metal complexes. *Energies* **2021**, *14*, 1334. [CrossRef]
5. Navlani-García, M.; Salinas-Torres, D.; Cazorla-Amorós, D. Hydrogen production from formic acid attained by bimetallic heterogeneous PdAg catalytic systems. *Energies* **2019**, *12*, 4027. [CrossRef]

6.   Joó, F. Breakthroughs in Hydrogen Storage—Formic Acid as a Sustainable Storage Material for Hydrogen. *ChemSusChem* **2008**, *1*, 805–808. [CrossRef]

7.   Loges, B.; Boddien, A.; Gärtner, F.; Junge, H.; Beller, M. Catalytic Generation of Hydrogen from Formic acid and its Derivatives: Useful Hydrogen Storage Materials. *Top. Catal.* **2010**, *53*, 902–914. [CrossRef]

8.   Valentini, F.; Kozell, V.; Petrucci, C.; Marrocchi, A.; Gu, Y.; Gelman, D.; Vaccaro, L. Formic acid, a biomass-derived source of energy and hydrogen for biomass upgrading. *Energy Environ. Sci.* **2019**, *12*, 2646–2664. [CrossRef]

9.   Gan, W.; Dyson, P.J.; Laurenczy, G. Hydrogen storage and delivery: Immobilization of a highly active homogeneous catalyst for the decomposition of formic acid to hydrogen and carbon dioxide. *React. Kinet. Catal. Lett.* **2009**, *98*, 205–213. [CrossRef]

10. Bhandari, S.; Rangarajan, S.; Maravelias, C.T.; Dumesic, J.A.; Mavrikakis, M. Reaction mechanism of vapor-phase formic acid decomposition over platinum catalysts: DFT, reaction kinetics experiments, and microkinetic modeling. *Acs Catal.* **2020**, *10*, 4112–4126. [CrossRef]

11. Wang, X.; Meng, Q.; Gao, L.; Jin, Z.; Ge, J.; Liu, C.; Xing, W. Recent progress in hydrogen production from formic acid decomposition. *Int. J. Hydrogen Energy* **2018**, *43*, 7055–7071. [CrossRef]

12. Younas, M.; Rezakazemi, M.; Arbab, M.S.; Shah, J.; Rehman, W.U. Green hydrogen storage and delivery: Utilizing highly active homogeneous and heterogeneous catalysts for formic acid dehydrogenation. *Int. J. Hydrogen Energy* **2022**, *47*, 11694–11724. [CrossRef]

13. Wang, X.; Meng, Q.; Gao, L.; Liu, J.; Ge, J.; Liu, C.; Xing, W. Metal organic framework derived nitrogen-doped carbon anchored palladium nanoparticles for ambient temperature formic acid decomposition. *Int. J. Hydrogen Energy* **2019**, *44*, 28402–28408. [CrossRef]

14. Ding, T.-Y.; Zhao, Z.-G.; Ran, M.-F.; Yang, Y.-Y. Superior activity of Pd nanoparticles confined in carbon nanotubes for hydrogen production from formic acid decomposition at ambient temperature. *J. Colloid Interface Sci.* **2019**, *538*, 474–480. [CrossRef]

15. Hafeez, S.; Harkou, E.; Spanou, A.; Al-Salem, S.M.; Villa, A.; Dimitratos, N.; Manos, G.; Constantinou, A. Review on recent progress and reactor set-ups for hydrogen production from formic acid decomposition. *Mater. Today Chem.* **2022**, *26*, 101120. [CrossRef]

16. Choi, B.-S.; Song, J.; Song, M.; Goo, B.S.; Lee, Y.W.; Kim, Y.; Yang, H.; Han, S.W. Core–shell engineering of Pd–Ag bimetallic catalysts for efficient hydrogen production from formic acid decomposition. *ACS Catal.* **2018**, *9*, 819–826. [CrossRef]

17. Zhang, Y.; Lyu, Y.; Wang, Y.; Li, C.; Jiang, M.; Ding, Y. Highly active and stable porous polymer heterogenous catalysts for decomposition of formic acid to produce H_2. *Chin. J. Catal.* **2019**, *40*, 147–151. [CrossRef]

18. Barlocco, I.; Capelli, S.; Lu, X.; Bellomi, S.; Huang, X.; Wang, D.; Prati, L.; Dimitratos, N.; Roldan, A.; Villa, A. Disclosing the role of gold on palladium–gold alloyed supported catalysts in formic acid decomposition. *ChemCatChem* **2021**, *13*, 4210–4222. [CrossRef]

19. Winkler, T.; Baccot, F.; Eränen, K.; Wärnå, J.; Hilpmann, G.; Lange, R.; Peurla, M.; Simakova, I.; Grénman, H.; Murzin, D.Y. Catalytic decomposition of formic acid in a fixed bed reactor—An experimental and modelling study. *Catal. Today* **2022**, *387*, 128–139. [CrossRef]

20. Hafeez, S.; Sanchez, F.; Al-Salem, S.M.; Villa, A.; Manos, G.; Dimitratos, N.; Constantinou, A. Decomposition of additive-free formic acid using a pd/c catalyst in flow: Experimental and cfd modelling studies. *Catalysts* **2021**, *11*, 341. [CrossRef]

21. Hafeez, S.; Barlocco, I.; Al-Salem, S.M.; Villa, A.; Chen, X.; Delgado, J.J.; Manos, G.; Dimitratos, N.; Constantinou, A. Experimental and process modelling investigation of the hydrogen generation from formic acid decomposition using a pd/zn catalyst. *Appl. Sci.* **2021**, *11*, 8462. [CrossRef]

22. Caiti, M.; Padovan, D.; Hammond, C. Continuous Production of Hydrogen from Formic Acid Decomposition over Heterogeneous Nanoparticle Catalysts: From Batch to Continuous Flow. *ACS Catal.* **2019**, *9*, 9188–9198. [CrossRef]

23. Xu, R.; Lu, W.; Toan, S.; Zhou, Z.; Russell, C.K.; Sun, Z.; Sun, Z. Thermocatalytic formic acid dehydrogenation: Recent advances and emerging trends. *J. Mater. Chem. A* **2021**, *9*, 24241–24260. [CrossRef]

24. Wang, Z.; Ashok, J.; Pu, Z.; Kawi, S. Low temperature partial oxidation of methane via BaBi0. 05Co0. 8Nb0. 15O3− δ-Ni phyllosilicate catalytic hollow fiber membrane reactor. *Chem. Eng. J.* **2017**, *315*, 315–323. [CrossRef]

25. Shahbaz, M.; Al-Ansari, T.; Aslam, M.; Khan, Z.; Inayat, A.; Athar, M.; Naqvi, S.R.; Ahmed, M.A.; McKay, G. A state of the art review on biomass processing and conversion technologies to produce hydrogen and its recovery via membrane separation. *Int. J. Hydrogen Energy* **2020**, *45*, 15166–15195. [CrossRef]

26. Cechetto, V.; Di Felice, L.; Medrano, J.A.; Makhloufi, C.; Zuniga, J.; Gallucci, F. H_2 production via ammonia decomposition in a catalytic membrane reactor. *Fuel Process. Technol.* **2021**, *216*, 106772. [CrossRef]

27. Hafeez, S.; Al-Salem, S.M.; Bansode, A.; Villa, A.; Dimitratos, N.; Manos, G.; Constantinou, A. Computational Investigation of Microreactor Configurations for Hydrogen Production from Formic Acid Decomposition Using a Pd/C Catalyst. *Ind. Eng. Chem. Res.* **2022**, *61*, 1655–1665. [CrossRef]

28. Hafeez, S.; Aristodemou, E.; Manos, G.; Al-Salem, S.M.; Constantinou, A. Computational fluid dynamics (CFD) and reaction modelling study of bio-oil catalytic hydrodeoxygenation in microreactors. *React. Chem. Eng.* **2020**, *5*, 1083–1092. [CrossRef]

29. Hafeez, S.; Aristodemou, E.; Manos, G.; Al-Salem, S.M.; Constantinou, A. Modelling of packed bed and coated wall microreactors for methanol steam reforming for hydrogen production. *RSC Adv.* **2020**, *10*, 41680–41692. [CrossRef]

30. Hafeez, S.; Al-Salem, S.M.; Manos, G.; Constantinou, A. Fuel production using membrane reactors: A review. *Environ. Chem. Lett.* **2020**, *18*, 1477–1490. [CrossRef]

31. Harkou, E.; Hafeez, S.; Manos, G.; Constantinou, A. CFD Study of the Numbering up of Membrane Microreactors for CO_2 Capture. *Processes* **2021**, *9*, 1515. [CrossRef]

32. Wu, G.; Cao, E.; Ellis, P.; Constantinou, A.; Kuhn, S.; Gavriilidis, A. Development of a flat membrane microchannel packed-bed reactor for scalable aerobic oxidation of benzyl alcohol in flow. *Chem. Eng. J.* **2019**, *377*, 120086. [CrossRef]

33. Constantinou, A.; Wu, G.; Venezia, B.; Ellis, P.; Kuhn, S.; Gavriilidis, A. Aerobic Oxidation of Benzyl Alcohol in a Continuous Catalytic Membrane Reactor. *Top. Catal.* **2019**, *62*, 1126–1131. [CrossRef]

34. Sanchez, F.; Motta, D.; Roldan, A.; Hammond, C.; Villa, A.; Dimitratos, N. Hydrogen generation from additive-free formic acid decomposition under mild conditions by Pd/C: Experimental and DFT studies. *Top. Catal.* **2018**, *61*, 254–266. [CrossRef] [PubMed]

35. Wang, Y.; Qi, Y.; Zhang, D.; Liu, C. New Insight into the Decomposition Mechanism of Formic Acid on Pd(111): Competing Formation of CO_2 and CO. *J. Phys. Chem. C* **2014**, *118*, 2067–2076. [CrossRef]

36. Kosider, A.; Blaumeiser, D.; Schötz, S.; Preuster, P.; Bösmann, A.; Wasserscheid, P.; Libuda, J.; Bauer, T. Enhancing the feasibility of Pd/C-catalyzed formic acid decomposition for hydrogen generation–catalyst pretreatment, deactivation, and regeneration. *Catal. Sci. Technol.* **2021**, *11*, 4259–4271. [CrossRef]

37. Sandoval, V.H.; Gigola, C.E. Characterization of Pd and Pd Pbα-Al_2O_3 catalysts. A TPR-TPD study. *Appl. Catal. A Gen.* **1996**, *148*, 81–96. [CrossRef]

38. Richardson, J.; Harker, J.; Backhurst, J. Flow of fluids through granular beds and packed columns. *Chem. Eng.* **2002**, *2*, 191–236.

39. Fogler, H.S. *Elements of Chemical Reaction Engineering*, 3rd ed.; Prentice Hall PTR: Upper Saddle River, NJ, USA, 1999. Available online: https://search.library.wisc.edu/catalog/999810177702121 (accessed on 10 June 2023).

40. Froessling, N. Über die verdunstung fallender tropfen. *Gerlands Beiträge Zur Geophys.* **1938**, *52*, 170–216.